Plant Mol Biol (2011) 77:447–459
DOI 10.1007/s11103-011-9823-8

Initial characteristics of RbcX proteins from *Arabidopsis thaliana*

Piotr Kolesiński · Janusz Piechota · Andrzej Szczepaniak

Received: 24 February 2011 / Accepted: 24 August 2011 / Published online: 16 September 2011

Abstract Form I of Rubisco (ribulose-1,5-bisphosphate carboxylase/oxygenase) is composed of eight large (RbcL) and eight small (RbcS) subunits. Assembly of these subunits into a functional holoenzyme requires the assistance of additional assembly factors. One such factor is RbcX, which has been demonstrated to act as a chaperone in the assembly of most cyanobacterial Rubisco complexes expressed in heterologous system established in *Escherichia coli* cells. Analysis of *Arabidopsis thaliana* genomic sequence revealed the presence of two genes encoding putative homologues of cyanobacterial RbcX protein: *AtRbcX1* (*At4G04330*) and *AtRbcX2* (*At5G19855*). In general, both RbcX homologues seem to have the same function which is chaperone activity during Rubisco biogenesis. However, detailed analysis revealed slight differences between them. AtRbcX2 is localized in the stromal fraction of chloroplasts whereas AtRbcX1 was found in the insoluble fraction corresponding with thylakoid membranes. Search for putative "partners" using mass spectrometry analysis suggested that apart from binding to RbcL, AtRbcX1 may also interact with β subunit of chloroplast ATP synthase. Quantitative RT-PCR analysis of *AtRbcX1* and *AtRbcX2* expression under various stress conditions indicated that *AtRbcX2* is transcribed at a relatively stable level, while the transcription level of *AtRbcX1* varies significantly. In addition, we present the attempts to elucidate the secondary structure of AtRbcX proteins using CD spectroscopy. Presented results are the first known approach to elucidate the role of RbcX proteins in Rubisco assembly in higher plants.

Keywords RbcX · Rubisco assembly · *Arabidopsis thaliana*

Abbreviations

qRT-PCR	Quantitative reverse transcription polymerase chain reaction
CD	Circular dichroism

Introduction

Ribulose-1,5-bisphosphate carboxylase/oxygenase (Rubisco, EC 4.1.1.39) catalyses the addition of CO_2 to ribulose-1,5-bisphosphate (RuBP) resulting in the formation of unstable six-carbon compound cleaved later into two molecules of 3-phosphoglyceric acid (for review see Cleland et al. 1998). This reaction, being the only quantitatively significant link between the pools of inorganic carbon dioxide and organic matter of the biosphere, is the slowest and therefore the rate-limiting step of photosynthesis. Apart from CO_2 fixation, Rubisco is capable of introducing O_2 into RuBP during the photorespiration reaction (Bowes et al. 1971). Photorespiration decreases the effectiveness of CO_2 assimilation. As photorespiration is considered one of the major factors limiting biomass production by plants, many attempts have been made to

Electronic supplementary material The online version of this article (doi:10.1007/s11103-011-9823-8) contains supplementary material, which is available to authorized users.

P. Kolesiński · A. Szczepaniak (✉)
Laboratory of Biophysics, Faculty of Biotechnology, University of Wroclaw, Przybyszewskiego 63/77, 51-148 Wroclaw, Poland
e-mail: andrzej.szczepaniak@ibmb.uni.wroc.pl

J. Piechota
Laboratory of Cellular Molecular Biology, Faculty of Biotechnology, University of Wroclaw, Przybyszewskiego 63/77, 51-148 Wroclaw, Poland

refine Rubisco properties in this aspect. Thus far, only a few mutations in cyanobacterial Rubisco have led to an increased carbon fixation velocity or increased affinity to carbon dioxide instead of oxygen (Mueller-Cajar and Whitney 2008; Smith and Tabita 2003). Although, some attempts to improve the properties this enzyme in higher plants have been made (Whitney et al. 1999), the progress in this field is limited due to the lack of a simple method for effective screening towards desired amino acid substitutions.

Form I of Rubisco found in cyanobacteria, green algae as well as in lower and higher plants is a holoenzyme that consists of eight large (RbcL) and eight small (RbcS) subunits. Large subunits with molecular masses of ~50 kDa form the core of the enzyme—tetramer of anti-parallel catalytic dimers. The core is capped at the top and the bottom by small subunits with masses of ~15 kDa. Assembly of RbcL and RbcS subunits into the functional holoenzyme needs the assistance of certain folding and assembly factors such as GroEL and RbcX. Cyanobacterial Rubisco is encoded by an operon consisting of *rbcL* and *rbcS* genes separated by *rbcX* gene. Protein product of *rbcX* is required for proper Rubisco biosynthesis (Onizuka et al. 2004; Li and Tabita 1997). Interestingly, in two strains of cyanobacterial species—*Synechococcus* sp. PCC6301 (Goloubinoff et al. 1989) and *Synechococcus* sp. PCC7942 (Emlyn-Jones et al. 2006)—RbcX is unnecessary for Rubisco assembly and its gene is localized outside the Rubisco operon. Recently, it has been demonstrated that cyanobacterial RbcL protein is folded by the GroEL/GroES complex and retains high affinity for this chaperonin until its C-terminal fragment is captured by the RbcX dimer (Liu et al. 2010). After the release of RbcL from GroEL, RbcX stabilizes RbcL dimers and facilitates the $RbcL_8$ core assembly. Incorporation of RbcS into holoenzyme results in a decreased affinity of RbcX to RbcL, which leads to the release of C-terminal fragment of the large subunit and formation of fully functional Rubisco enzyme.

Mechanism of Rubisco biosynthesis in plants is even more complex and not yet fully understood. Large subunit of plant Rubisco is encoded by chloroplast *rbcL* gene, whereas a family of *RBCS* genes is localized in the nucleus. Because large and small subunits of plant Rubisco are encoded by two different genomes and their synthesis is spatially separated, a sophisticated mechanism is required to harmonize/synchronize the synthesis of these subunits with their assembly into a functional holoenzyme. The existence of such a mechanism has been recently reported (Whitney et al. 2009). Translation of RbcL, like the majority of chloroplast proteins, is regulated by epistasy of synthesis (Wostrikoff and Stern 2007). Similar to cyanobacteria, proper folding of plant RbcL subunit requires the presence of certain chaperones, i.e. Cpn60 that can stimulate the folding (but not the assembly) of plant large Rubisco subunit during its expression in *Escherichia coli* (Cloney et al. 1993). Additional proteins, such as BSD2 chaperone (identified in the study of a maize mutant that fails to accumulate Rubisco), may also be engaged in the Rubisco biosynthesis process (Brutnell et al. 1999).

Analysis of successively sequenced plant genomes such as *Arabidopsis thaliana*, maize (*Zea mays*), rice (*Oryza sativa*) and *Sorghum bicolor* reveals the presence of nuclear-localized genes encoding homologs of cyanobacterial RbcX proteins in these species. In *Arabidopsis* genome, two such homologs are localized: *At4G04330* and *At5G19855*. Our studies focus on preliminary characterization of these genes and the proteins encoded by them. We investigated the activity of both proteins in the Rubisco assembly process, their cellular localization and secondary structure. Expression of both genes under various stress conditions was also analyzed. To our knowledge, this is the first report that describes higher plant RbcX proteins and elucidates their role in the Rubisco biosynthesis process.

Results and discussion

Identification of RbcX proteins in *Arabidopsis thaliana* genome

The main goal of our study was to identify the chaperone involved in Rubisco assembly process (RbcX protein) in plant chloroplasts. Analysis of *Arabidopsis* genome revealed the presence of two genes encoding putative RbcX proteins. Predicted protein product of the *At4G04330* gene (called further in this study AtRbcX1) shares 28% overall sequence similarity with RbcX from marine cyanobacteria *Synechococcus* sp. PCC 7002, whereas protein product of the *At5G19855* gene (called further AtRbcX2) shows 15% overall similarity with this cyanobacterial protein. Alignment of selected cyanobacterial RbcX protein sequences with plant homologs (Supplemental Fig. S1) revealed the presence of additional 50–80 amino acids at the N-termini of *Arabidopsis* proteins. We believe that these additional N-terminal sequences are transit peptides, because most of the targeting sequence prediction algorithms identified AtRbcX1 and AtRbcX2 as chloroplast-targeted proteins. However, no unequivocal indication for stromal protease cleavage site was obtained.

Based on the chosen cyanobacterial RbcX sequences and majority of their predicted homologs in lower (*Physcomitrella patens*) and higher plants including gymnosperm (*Picea sitchensis*) and angiosperms (*Vitis vinifera*, *Populus trichocarpa*, *Zea mays*, *Sorghum bicolor*, *Ricinus communis*, *Oryza sativa* and *Arabidopsis thaliana*), a phylogenetic tree was generated using BLOSUM matrix

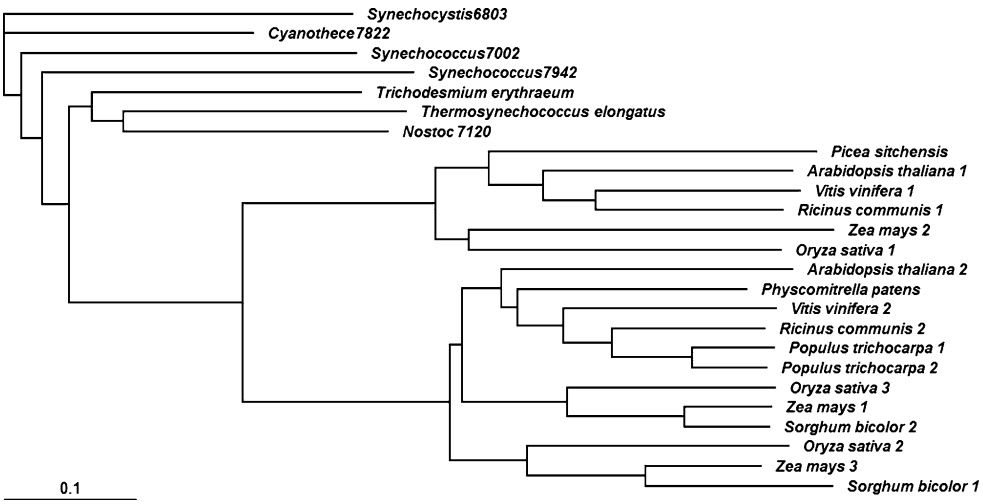

Fig. 1 Phylogenetic analysis of RbcX proteins from cyanobacteria and lower and higher plants

(Fig. 1). Phylogenetic analysis indicated that plant RbcXs evolved from their cyanobacterial ancestors. During evolution at least one duplication of plant *rbcX* genes occurred. However, it is impossible to identify the exact timeline of the duplication because of limited number of plant RbcXs sequences. As a result of this duplication, most plants have at least two versions of the *rbcX* gene. Only one identified copy of the *rbcX* gene is present in the genome of *Physcomitrella patens* and *Picea sitchensis*.

Chloroplast localization of AtRbcX proteins

The chaperone activity of cyanobacterial RbcX proteins in Rubisco biogenesis has already been demonstrated in *E. coli* system, therefore we expected to find their higher-plants counterparts in chloroplasts, where the biosynthesis of plant Rubisco occurs. In order to confirm this theory, we constructed transgenic *A. thaliana* plants expressing *AtRbcX* genes supplemented with C-terminal Strep-Tag II encoding sequences under the control of CaMV 35S promoter. Two pCambia1302 plasmids with cloned open reading frames of AtRbcX1 and AtRbcX2 proteins with attached Strep-tags on their C-termini (named pCamX1ST and pCamX2ST, respectively) were used for *Agrobacterium*-mediated transformation of the wild type *Arabidopsis*. Five and seven hygromycin-resistant plantlets were selected after transformation with pCamX1ST and pCamX2ST plasmids, respectively. Integration of the transgenes into the *Arabidopsis* genome was confirmed by PCR with primers flanking *AtRbcX* gene cloning region of pCambia 1302 vector (Supplemental Fig. S2). Seeds obtained from line 3 of pCamX1ST transformants and line 6 of pCamX2ST transformants were used in further experiments.

Chloroplasts from ca. 8-weeks-old rosettes of transformants and wild type plants were isolated and fractionated into thylakoid and stromal fractions (Fig. 2a). Immunodetection with Anti-Strep-Tag II antibodies indicated that both proteins were present in the chloroplasts of transformed plants (Fig. 2b). Subfractionation of chloroplasts showed that AtRbcX2ST protein mostly localizes in the stromal fraction which corresponds with Rubisco localization. Surprisingly, AtRbcX1ST protein was found in the thylakoid fraction. In order to determine the nature of the interaction of AtRbcX1ST protein with thylakoid membranes, thylakoid fraction was washed with NaCl, CAPS or Triton X-100. All of these treatments remove peripheral but not integral membrane proteins. In all the cases, AtRbcX1ST protein was found in the pellet fraction (Fig. 2c).

In silico analysis of AtRbcX1ST sequence did not indicate the presence of trans-membrane domains, suggesting other type of interaction between AtRbcX1 and thylakoid membrane. It has been reported that RbcL is translated on polysomes bound to thylakoid membranes (Muehlbauer and Eichacker 1999). Nevertheless, in that study Rubisco was washed out effectively from the membrane fraction even in the presence of 0.5 M KCl which eliminates any chance that AtRbcX1 protein interacts with thylakoids indirectly through large Rubisco subunit synthesized on membrane-bound ribosomes. It is conceivable that AtRbcX1 protein can interact by hydrophobic or covalent bond with membrane-localized protein other than Rubisco. Some proteins may be anchored to the membrane by acyl residue attached during post-translational modification, i.e. palmitoylation or myristoylation. However, such modifications are not common amongst the chloroplast proteins. Analysis of mature AtRbcX1 polypeptide-using in silico tools that predict palmitoylation and myristoylation did not indicate the presence of such modifications in the investigated protein. Further attempts to express the processed AtRbcX1ST protein in *E. coli* cells revealed that this polypeptide demonstrate limited

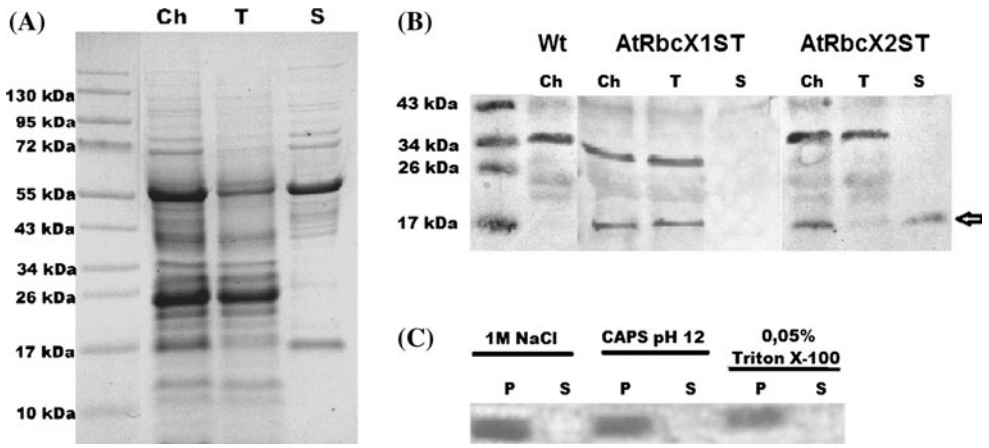

Fig. 2 Localization of AtRbcXST proteins in *Arabidopsis* chloroplasts. Chloroplasts were isolated from wild type (Wt) plants and from transformed plants expressing AtRbcX1ST or AtRbcX2ST proteins. Thylakoid or stromal fractions were obtained from chloroplasts of transformed plants. Samples of chloroplasts (Ch) and thylakoid (T) and stromal (S) fractions were separated by Tricine-PAGE and Coomassie-stained or transferred to nitrocellulose membrane and probed with anti-Strep Tag II antibodies. **a** Coomassie staining of separated proteins; **b** Immunodetection of Strep-tagged AtRbcX1 and AtRbcX2 proteins in plants transformed with pCam-rbcX1 or pCam-rbcX2 constructs. The *arrow* indicates the band corresponding to Strep-tagged AtRbcX proteins; **c** Thylakoids from plants expressing Strep-tagged AtRbcX1 protein were resuspended in 1 M NaCl, 20 mM CAPS pH 12 or 0.05% Triton X-100, incubated for 1 h and centrifuged. Proteins present in pellets (P) or supernatants (S) were separated by 10% SDS–PAGE, transferred to nitrocellulose membrane and probed with anti-Strep Tag II antibodies

solubility in comparison with its untagged variant (Supplemental Fig. S3). Thus, the presence of AtRbcX1ST protein in pelleted thylakoid fraction may also result from its decreased solubility. Because of relatively low level of AtRbcX proteins in chloroplasts, it is difficult to confirm their exact localization in this organelle due to limitations in the detection method.

Identification of proteins interacting with AtRbcX1 and AtRbcX2

Additional Strep-Tag II sequence introduced at the end of AtRbcX proteins enabled their purification from *A. thaliana* leaf extracts by binding them to commercially available Strep-Tactin resin. Proteins eluted from resin using biotin-containing buffer were separated by Tricine-PAGE (Fig. 3) and identified by mass spectroscopy. The results are summarized in Table 1. In order to identify proteins interacting non-specifically with Strep-Tactin resin, we conducted additional purification using *Arabidopsis* wild type leaves. This approach led to the identification of two non-specifically bound proteins which were LHCB5 (LIGHT HARVESTING COMPLEX OF PHOTOSYSTEM II 5), found also in from X2ST plantlets eluate (and tightly bound to Strep-Tactin in case of X1ST), and biotinylated ACC1 (ACETYL-COENZYME A CARBOXYLASE 1) found in all investigated eluates. Our experiment confirmed the presence of tagged AtRbcX peptides in eluates from Strep-Tactin resin. Moreover, analysis of gel fragments containing additional bands enabled us to recognize putative "partners" of AtRbcX proteins. As we expected, both investigated proteins interact with large Rubisco subunit. The additional protein identified in the eluates from both types of transgenic plants was THI1. This enzyme with the molecular mass of ca. 35 kDa is targeted to chloroplasts and mitochondria and is involved in oxazole or thiazole synthesis (Belanger et al. 1995). Its connection with RbcX proteins is not clear yet.

Some polypeptides were found in eluates of only one type of transgenic plants. Thus, these polypeptides may represent proteins specifically interacting with AtRbcX1 or AtRbcX2. Analysis of the gel fragment containing AtRbcX2ST also revealed the presence of protein F1019.10 (Rubisco small subunit 1B). Surprisingly, AtRbcX1ST co-purified with a significant amount of β subunit of ATP synthase CF1. This synthase is localized in the thylakoid membrane. Thus, interaction between CF1 ATPase and AtRbcX1 indicates toward their co-localization in the same compartment. However, there is no similarity in the C-terminal RbcL sequence interacting with RbcX (Saschenbrecker et al. 2007) to any fragment of β subunit of ATP synthase CF1. This chloroplast ATP synthase is a multisubunit enzyme and after heterologous expression in *E. coli* cells, it was reported to be present only in inclusion bodies. Its proper refolding and reconstitution required a mix of chloroplast chaperones isolated from spinach (Chen and Jagendorf 1994). Similar to Rubisco of higher plants, bacterial chaperone GroEL/GroES was not sufficient for proper folding of CF1 ATPase in bacterial host. It is conceivable that during evolution, one of the duplicated AtRbcX

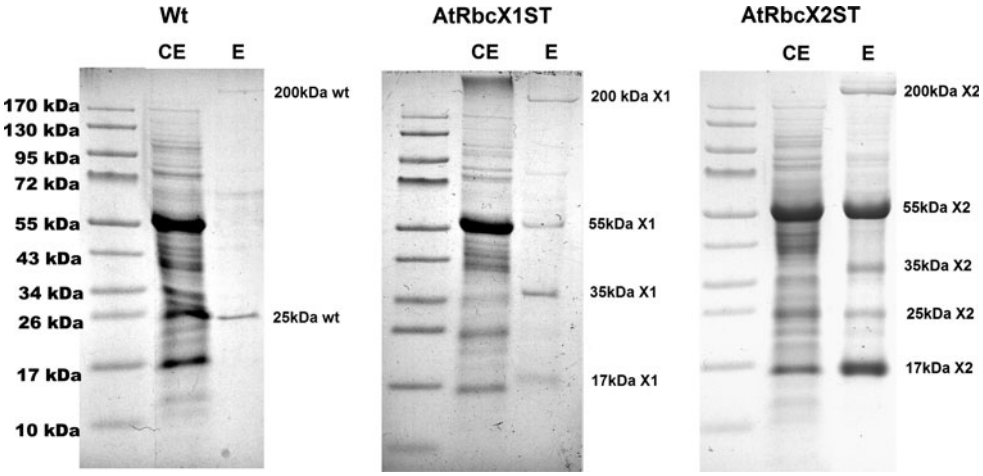

Fig. 3 Tricine-PAGE analysis of protein bounded to Strep-Tactin resin extracted from wild type (Wt), X1ST (AtRbcX1ST) and X2ST (AtRbcX2ST) *A. thaliana* leaves. Lanes indicated as "CE" contain 20 μg of total leaf proteins whereas those indicated as "E" contain eluates from Strep-Tactin being equivalent of 10 g of wild type and X2ST leaves and 5 g of X1ST leaves, respectively

Table 1 Identification of proteins eluted from Strep-Tactin resin by mass spectroscopy

	Protein name	gi number	TAIR number
200 kDa wt	ACC1	gil79358114	At1g36160
25 kDa wt	LHCB5	gil15235029	At4g10340
200 kDa X1	ACC1	gil79358114	At1g36160
55 kDa X1	RbcL	gil7525041	ArthCp030
	ATP synthase CF1 β subunit	gil7525040	ArthCp029
35 kDa X1	THI1	gil15239735	At5g54770
17 kDa X1	AtRbcX1	gil18412539	At4g04330
200 kDa X2	ACC1	gil79358114	At1g36160
55 kDa X2	RbcL	gil7525041	ArthCp030
35 kDa X2	THI1	gil15239735	At5g54770
25 kDa X2	LHCB5	gil15235029	At4g10340
17 kDa X2	AtRbcX2	gil18420050	At5g19855
	F1019.10	gil13926229	At5g38430

proteins gained an additional function of assisting in CF1 ATPase assembly or folding. Interestingly, no trace of AtRbcX2 protein was found in the preparation from X1ST *Arabidopsis* plants and vice versa. Of course, this observation does not exclude weak binding or possible interaction requiring an unidentified co-factor. Also, it is conceivable that steric hindrances, after binding to Strep-Tactin resin, could prevent the binding of AtRbcX proteins to each other. Nevertheless, this fact may also suggest that AtRbcX1 and AtRbcX2 neither cooperate with each other during synthesis of one Rubisco complex nor do they interact with each other directly.

Proteins eluted from Strep-Tactin column and then separated by employing Tricine-PAGE were also transferred onto PVDF membrane. Membrane-bound proteins from fragments indicated as "17 kDa X1" and "17 X2" were subjected to N-terminus sequencing by Edman degradation. Identified N-terminal sequences of mature AtRbcX1 and AtRbcX2 proteins were KMYVP and EDVAG, respectively. This indicates that AtRbcX1 preprotein is cleaved after 45th amino acid of the signal sequence and AtRbcX2 preprotein is cleaved after the 78th amino acid. Lengths of signal sequences of these proteins are within the typical length of chloroplast targeting sequences consisting usually of 30–80 residues (Zhang and Glaser 2002). However, the presence of asparagine at −1 position of cleavage site of both preproteins is quite unusual as generally small and hydrophobic residues (like Ala or Gly) are preferred (Dalbey et al. 1997). Predicted molecular weights of processed Strep-tagged peptides are 16,051 Da for AtRbcX1 and 15,958 Da for AtRbcX2, which corresponds with positions of these proteins on proteinograms. Stromal protease cleavage sites determined by Edman degradation differs from those indicated by algorithms predicting signal sequences such as TargetP and ChloroP (predicted cleavage site after 58th amino acid of AtRbcX1 and 62th amino acid of AtRbcX2 protein) and SignalP (predicted cleavage site after 23th amino acid of AtRbcX2 and no indication of cleavage site for AtRbcX1). Variants of AtRbcX proteins with removed signal peptides indicated by these algorithms

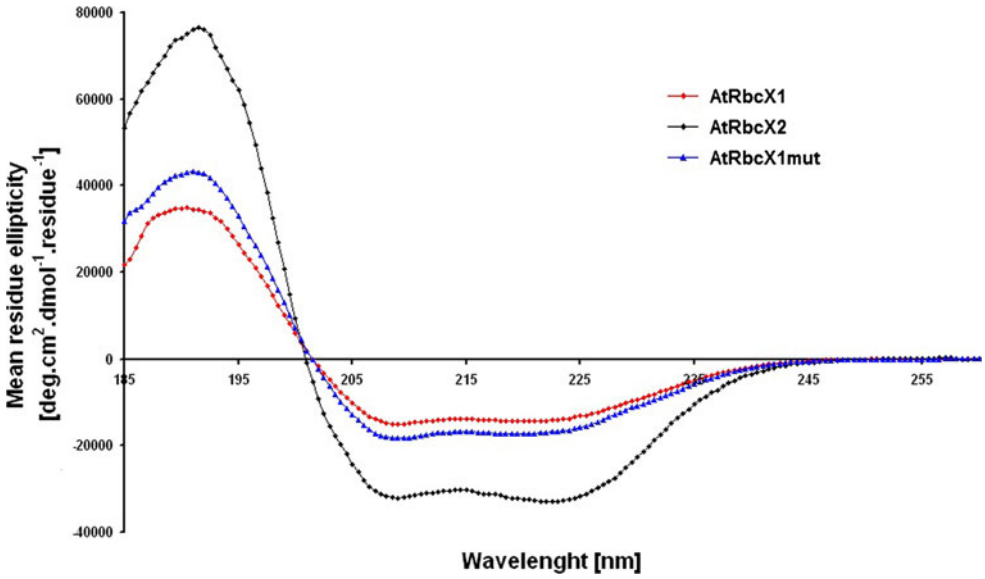

Fig. 4 Far UV–CD spectra of purified recombinant AtRbcX proteins. AtRbcX1 (wild type and mutated) and AtRbcX2 proteins lacking signal peptides were expressed in *E. coli* Rosetta strain and purified. CD spectra of purified proteins were analyzed in the range of 185–260 nm using Jasco J-815 spectropolarimeter

show very limited solubility when expressed in *E. coli*. Nevertheless, the variants predicted by SignalP algorithm exhibit chaperone activity in cyanobacterial Rubisco biosynthesis in *E. coli* cells (data not shown).

Purification and secondary structure analysis of recombinant AtRbcX proteins

To analyze the secondary structure of AtRbcX proteins, both polypeptides, without identified signal sequences, were expressed in *E. coli* and purified. In order to do this, appropriate fragments of open reading frames corresponding to mature proteins were cloned into pET21b vector with simultaneous elimination of His-Tag sequence present in this vector giving pET21rbcX1pr and pET21rbcX2pr plasmids. In the case of AtRbcX1 protein, we removed the first 46 amino acids instead of 45. Because the second residue in mature polypeptide is a methionine, we decided to omit the first lysine codon instead of introducing an additional start codon. Yields of protein purifications were about 3 mg per l of bacterial culture for AtrbcX1 and ca. 0.2 mg per l of bacterial culture for AtRbcX2. Circular dichroism spectra measurements were performed for purified proteins (Fig. 4). According to earlier predictions, AtRbcX2 protein contains mainly α-helices and small number of turns and unordered structures. Structures of RbcX proteins from *Synechococcus* sp. PCC7002 and *Anabaena* CA. already deposed in Protein Data Bank (PDB, http://www.rcsb.org/pdb/home/home.do) demonstrate almost the same contribution of α-helices, β-turns and random coil as AtRbcX2 protein (see Table 2). In opposition to AtRbcX2, purified recombinant AtRbcX1 protein had the tendency to aggregate (indicated by the presence of non-denatured "dimer" even in denaturing polyacrylamide gel). Since it has been reported that the presence of cysteine residue in RbcX protein may lead to its aggregation (Tarnawski et al. 2008b), we decided to replace both cysteines present in AtRbcX1 protein with amino acids present in corresponding positions in cyanobacterial RbcXs introducing C62L and C87A mutations. Mutated AtRbcX1 was found in high amounts in soluble fraction and was purified in only one step (Supplemental Fig. S4C), resulting in ca. 20 mg protein per l of bacterial culture, with purity of more than 95%. Analysis of CD spectra indicated only slight changes in the structure of mutated AtRbcX1 as compared with wild type protein. Both wild type and mutated AtRbcX1 proteins mainly consist of α-helices, but their amounts are significantly lower than in already crystallized cyanobacterial RbcX homologs. Relatively high amount of β-strand predicted by CD spectra analysis is also unusual among cyanobacterial proteins. Additional structural studies are required to indicate the main differences between cyanobacterial and plant RbcX proteins. In opposition to wild type variant, mutated AtRbcX1 does not show a tendency to aggregation, which makes this protein a good subject for further crystallization experiments.

Chaperone activity of AtRbcX proteins

To verify whether RbcX proteins from *A. thaliana* show any chaperone activity during Rubisco synthesis process in *E. coli* cells, we co-expressed genes encoding AtRbcX1 or AtRbcX2 protein without signal peptide (with N-terminus indicated by Edman degradation) carried on one plasmid with genes encoding the large and small subunit of Rubisco present on a separate plasmid. In our experiments, we used Rubisco from thermophilic cyanobacteria *Thermosynechococcus elongatus* BP-1 because until now any attempt to obtain active higher-

Table 2 Data deconvolution of AtRbcX1, AtRbcX1mut and AtRbcX2, using Selcon3, CONTIN and CDSSTR methods

Distributions of structural components in two exemplary cyanobacterial RbcX structures already deposed in PDB are listed above

Average values obtained using Selcon3, CONTIN and CDSSTR algorithms as well as contribution of secondary structure elements in already crystallized cyanobacterial RbcX proteins are bolded

		Helix	Strand	Turn	Unordered
AtRbcX1	Selcon3	0.45	0.14	0.16	0.25
	CONTIN	0.44	0.14	0.14	0.27
	CDSSTR	0.48	0.16	0.13	0.22
	Average	**0.46**	**0.15**	**0.14**	**0.25**
AtRbcX1mut	Selcon3	0.53	0.10	0.12	0.24
	CONTIN	0.57	0.07	0.10	0.26
	CDSSTR	0.58	0.12	0.10	0.20
	Average	**0.56**	**0.10**	**0.11**	**0.23**
AtRbcX2	Selcon3	0.88	0	0.03	0.16
	CONTIN	0.90	0	0.02	0.08
	CDSSTR	0.93	0	0.01	0.04
	Average	**0.90**	**0**	**0.02**	**0.09**
Synechoccocus PCC7002 (2pen)		**0.88**		**0.02**	**0.10**
Anabaena CA (3hyb)		**0.88**		**0.03**	**0.08**

plant Rubisco during expression in *E. coli* has failed (Cloney et al. 1993).

Co-expression of *AtRbcX* genes with synthetic (lacking *rbcX* gene) cyanobacterial Rubisco operon led to functional complementation of RbcX protein from *T. elongatus* indicated by proper folding of large Rubisco subunit and formation of the active enzyme (Fig. 5). Two control experiments were carried out. In the first one, Rubisco subunits were expressed without any *rbcX* gene which resulted in drastically decreased Rubisco activity in crude extracts and the amount of large Rubisco subunit in both crude extracts and *E. coli* lysate was barely detectable. In the second experiment, Rubisco subunits were co-expressed with the native TeRbcX protein. Rubisco activities in *E. coli* cells transformed with TeRbcX, AtRbcX1 and AtRbcX2 were comparable, indicating that both AtRbcX proteins exhibit chaperone activity in TeRubisco assembly similar to the activity of TeRbcX protein. The same experiment was conducted with Strep-tagged variants of AtRbcX proteins (Supplemental Fig. S5). Both tagged proteins exhibited chaperone activity resulting in 87% of Rubisco activity for AtRbcX1ST and 24% for AtRbcX2ST, respectively when compared to Rubisco activity in the presence of the TeRbcX. This result indicates that the presence of Strep-tag in AtRbcX2 protein significantly reduces its chaperone activity. However, Rubisco activity, in the system employed strongly depends on the expression yields of its components. Thus, direct comparison of chaperone activities between expressed variants of AtRbX proteins may be inadequate.

Influence of various stress conditions on transcription of *AtRbcX* genes

It is supposed that multiple gene duplications in plant genomes result from adaptation of plants to various environmental stimuli or stresses. Presence of more than one *RbcX* gene in genomes of higher and lower plants may suggest that proteins encoded by these genes play their roles under different environmental conditions or have additional functions apart from participating in the assembly of Rubisco complex. Transfer of ancestral *RbcX* gene from chloroplast genome to nucleus enabled the evolution of mechanisms regulating the expression of plant *RbcX* homologs at the transcriptional level. To verify whether transcription of *AtRbcX* genes depends on environmental conditions, we compared levels of *AtRbcX1* and *AtRbcX2* transcripts in *Arabidopsis* plants under various stress conditions. Leaves of 8-week-old plants were exposed to various conditions such as oxidative, salt, desiccation, heat shock, high light or cold stresses. Leaves kept in ambient light and temperature conditions were used as the control. Levels of *AtRbcX1* and *AtRbcX2* transcripts were assayed by quantitative RT-PCR. In addition, expression levels of three genes indicated by RefGenes tool in Genevestigator database: *At1g69340* (encoding appr-1-p processing enzyme), *At4g17640* (encoding casein kinase II β-chain) and *At5g51880* (encoding expressed protein with yet unknown function) were compared under all the experimental conditions. Because *At4g17640* and *At5g51880* genes showed the smallest variation in transcript levels under investigated conditions, we chose them to be the reference genes in this experiment. Quantities of *AtRbcX1* and *AtRbcX2* transcripts were normalized separately on two selected reference genes and the obtained results were combined together using geometric mean. The averaged results are depicted in Fig. 6. Levels of the *AtRbcX2* transcripts were relatively stable under applied stress conditions. On the contrary, expression of the *AtRbcX1* gene was strongly dependent on environmental conditions. Salt stress, desiccation and cold stress caused

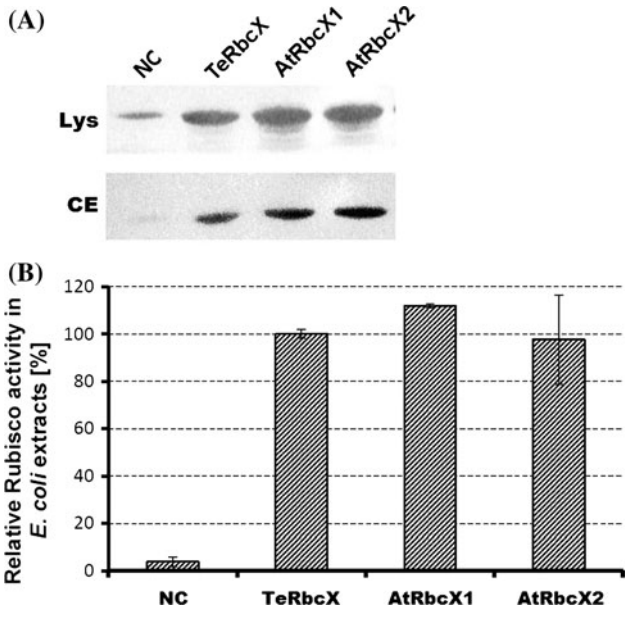

Fig. 5 Co-expression of *rbcL* and *rbcS* genes from *T. elongatus* BP-1 with *rbcX* genes from *A. thaliana*. Large and small Rubisco subunits of *Thermosynechococcus nongatus* BP-1 encoded by pUC18rbcLS plasmid were co-expressed with *AtRbcX1*, *AtRbcX2* or *T. elongatus RbcX* (*TeRbcX*, used as a positive control) encoded by pCM18 vector. Empty pCM18 vector was used as a negative control (NC). See "Materials and Methods" section for detailed description of used plasmids. **a** Western blot showing the presence of large Rubisco subunit from *T. elongatus* in *E. coli* lysates (Lys) and crude extracts (CE). Twenty μg of total proteins per line were separated by 10% Tricine-PAGE, transferred to nitrocellulose membrane, and probed with antibodies raised against large Rubisco subunit. **b** Comparison of Rubisco activity in crude *E. coli* extracts after co-expression experiments presented as percentage of Rubisco activity obtained after the co-expression of pUC18rbcLS and pCMrbcXTe plasmids. Data presented as mean ± SE are representative of three independent experiments

significant 6–12-fold increase in *AtRbcX1* transcript level, whereas oxidative stress resulted in twofold decrease in the level of this transcript. Changes in *AtRbcX1* transcript level observed in desiccation and salt stress are statistically significant ($P < 0.05$).

Presented results suggest that AtRbcX1 protein plays a compensating role in the assembly of Rubisco (or/and other protein complexes, e.g. chloroplast ATP synthase CF1), whereas AtRbcX2 seems to have a house-keeping role. Low temperatures, salinity and drought conditions initially lead to stomatal closure (Flexas and Medrano 2002) followed by decrease in both photosynthesis rate and quantity of photosynthetic enzymes (Kohzuma et al. 2009). Increased light intensity and exposition to oxidizing agents (such as H_2O_2) results in intracellular oxidative stress. It has been reported that light- and chemical-induced oxidative stresses result in translation arrest of the large Rubisco subunit (Cohen et al. 2005). Thus, transcription of *AtRbcX1* gene is influenced by conditions that directly or indirectly affect Rubisco biosynthesis. However, the reason as to why certain stress conditions increase and the other conditions decrease the level of *AtRbcX1* transcript remains unknown.

Materials and methods

Analysis of RbcX amino acid sequences

List of RbcX sequences used for alignment was created based on the NCBI protein database (http://www.ncbi.nlm.nih.gov/protein?term=RbcX). Alignment and phylogenetic tree construction were performed using ClustalW2 algorithm (http://www.ebi.ac.uk/Tools/msa/clustalw2/, Higgins et al. 1996). NCBI reference numbers of analyzed sequences are as follows: cyanobacteria—*Synechococcus* sp. PCC 7002 (YP_001735041.1), *Synechocystis* sp. PCC 6803 (NP_442121.1), *Thermosynechococcus elongatus* BP-1 (NP_682295.1), *Trichodesmium erythraeum* IMS101 (YP_723870.1), *Cyanothece* sp. PCC 7822 (YP_003888133.1), *Synechococcus elongatus* PCC 7942 (YP_400552.1), *Nostoc* sp. PCC 7120 (NP_485565.1); lower plants—*Physcomitrella patens* (XM_001770631), higher plants—*Picea sitchensis* (EF082099), *Vitis vinifera* 1(XM_002264334), *Vitis vinifera* 2 (XM_002279127); *Populus trichocarpa* 1 (XM_002298366), *Populus trichocarpa* 2 (XM_002314038), *Zea mays* 1 (NM_001151259), *Zea mays* 2 (NM_001151262), *Zea mays* 3 (NM_001149483), *Sorghum bicolor* 1 (XM_002463010), *Sorghum bicolor* 2 (XM_002466198), *Ricinus communis* 1 (XM_002518383), *Ricinus communis* 2 (XM_002513456), *Oryza sativa* 1 (NM_001068372), *Oryza sativa* 2 (NM_001066574), *Oryza sativa* 3 (NM_001058181), *Arabidopsis thaliana* 1 (NP_567263.1) and *Arabidopsis thaliana* 2 (NP_568382.1). Subcellular localization and stromal protease cleavage sites were predicted with SignalP (http://www.cbs.dtu.dk/services/SignalP/), ChloroP (http://www.cbs.dtu.dk/services/ChloroP/), TargetP (http://www.cbs.dtu.dk/services/TargetP/, Emanuelsson et al. 2007) and Predotar (http://urgi.versailles.inra.fr/predotar/predotar.html, Small et al. 2004). Potential presence of transmembrane fragments in AtRbcX proteins was verified according to TMpred (http://www.ch.embnet.org/software/TMPRED_form.html, Hofmann and Stoffel 1993) and TMHMM (http://www.cbs.dtu.dk/services/TMHMM-2.0/, Krogh et al. 2001) algorithms. Putative palmitoylation site prediction in mature AtRbcX1 protein was performed with CSS-Palm 2.0 (http://csspalm.biocuckoo.org/, Ren et al. 2008). The presence of possible myristoylation sites in this peptide was verified using Myristoylator tool (http://expasy.org/tools/myristoylator/, Bologna et al. in press).

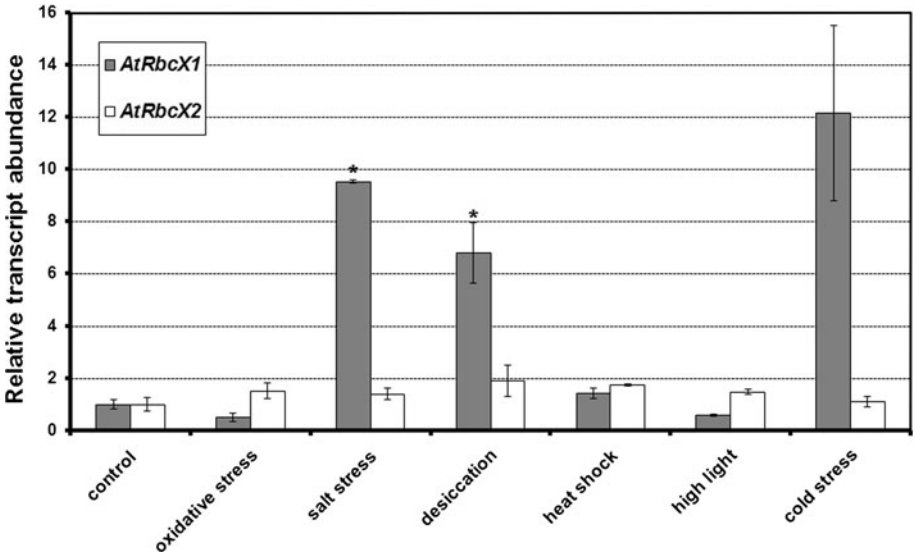

Fig. 6 Response of the *AtRbcX1* and *ArRbcX2* genes to selected stress conditions. RNA samples were obtained from leaves of wild type *Arabidopsis* plants subjected to various stress conditions for 2 h. Levels of *AtRbcX1* and *AtRbcX2* transcripts were quantified by qRT-PCR. Quantities of *AtRbcX1* and *AtRbcX2* transcripts normalized separately on *At4g17640* and *At5g51880* transcripts were combined together using geometric mean. The relative abundances of the *AtRbcX* transcripts in the control leaves were set as 1. Data are mean ± SE from three independent experiments. Results indicated by asterisks are statistically significant

Growth of plants and stress conditions

A. thaliana (ecotype Columbia 0) were grown in soil in an environmental chamber (Sanyo) at 22°C at a light intensity of 120 μmol × m^2 × s^{-1} under short-day conditions (8 h light/16 h dark).

All stress conditions were applied for 2 h to ca. 8-week-old rosettes transferred from soil to Petri dishes directly before experiment. Oxidative stress and salt stress were performed on rosettes floating on 2% H_2O_2 or on 0.4 M NaCl solutions, respectively. For cold or heat stress, rosettes floating on water were transferred to environmental chambers set at 4°C or 42°C. Desiccation stress was applied to rosettes dehydrated on 3 MM Whatman paper. For high light treatment, floating rosettes were transferred to environmental chamber set at light intensity of 220 μmol × m^2 × s^{-1}. Rosettes floating on water for 2 h under standard growth conditions were used as the control. Leaves from rosettes subjected to stress conditions and the control ones were used directly for RNA extraction.

Nucleic acids extraction and cDNA preparation

Total RNA was extracted from the control or stress-treated leaves using Tri Reagent (Sigma) according to the manufacturer's protocol. cDNA was synthesized using Revert Aid First Strand cDNA Synthesis Kit (Fermentas) and random hexamer primer.

Genomic DNA was isolated from *A. thaliana* using a GeneMATRIX Plant & Fungi DNA Purification Kit (EURx, Poland).

qRT-PCR analysis

After reverse transcription of 1 μg of total RNA, cDNA was diluted 10 times and 5 μl of this solution was used as a template for quantitative RT-PCR experiment. Maxima SYBR Green qPCR Master Mix (Fermentas) was used for qRT-PCR. All reactions were carried out in Roche LightCycler 2.0 (Roche) under following conditions: initial denaturation 10 min 95°C, 40 cycles of denaturation (15 s at 95°C), annealing (15 s at 60°C) and elongation (15 s at 72°C). Primers used for qRT-PCR were as follows:

X1RTFw CTCTCATGCGTCGCTCTTCAC3, X1RTRv TGTGTTGGAATCATCTACGTTCTTG (for *AtRbcX1*), X2RTFw AAGCTGTGAGGACGGTTCTTCATC, X2RTRv TTCTGCAAGCTCCTGACTCTCCTTG (for *AtRbcX2*), Ref1Fw GGAACAGTATTGTAGCTGAGGTAGC, Ref1Rv AACAACATCAGAACGGAACACATAC (for *At5g51880*—reference gene 1 gene encoding expressed protein), Ref2Fw GATGTGGAGTCTTCGCATGGTG, Ref2Rv ATTCCATATAGCATCTCTGCTGCTG (for *At4g17640*—reference gene 2, gene encoding casein kinase II *β*-chain), Ref3Fw TCATTCTGCAGCATCGTTACAA GTC and Ref3Rv TCGTTAAGATTGTAGCCTTCAA GTGG (for *At1g69340*—reference gene 3, gene encoding appr-1-p processing enzyme).

Reference genes in this experiment were indicated by Refgenes tool in Genevestigator database (https://www.genevestigator.ethz.ch/gv/index.jsp).

Construction of plasmids

For the transformation of *A. thaliana*, pCam-rbcX1ST and pCam-rbcX2ST plasmids were constructed by amplification of *AtRbcX1* gene using rbcX1STFw (AAACCATGG AGTCATCTTCTTCACTCC, *Nco*I site underlined) and rbcX1STRv (AAAGGTCACCTTA**TTTTTCGAACTGC GGGTGGCTCCA**CTTATCAGAATCGGTTTCG, *Eco*91I site underlined, Strep-Tag II encoding sequence in bold) primers and amplification of AtRbcX2 gene using rbcX2STFw (AAATCATGATGAGTGCTTGGTTTGTT GTTG, *Pag*I site underlined) and rbcX2STRv (AAAGG TCACCTTA**TTTTTCGAACTGCGGGTGGCTCCA**CC TTGAGTTTGTGTCATCGG, *Eco*91I site underlined, Strep-Tag II encoding sequence in bold) primers. PCR products digested with *Nco*I/*Eco*91I or *Pag*I/*Eco*91I, respectively were cloned into *Nco*I/*Eco*91I sites of pCambia1302 (Cambia) vector.

For the purification of AtRbcX proteins, deprived of signal peptides, from *E. coli* cells, suitable sequences were cloned into *Nde*I/*Bam*HI sites of pET21b vector (Invitrogen) giving pET21rbcX1pr and pET21rbcX2pr plasmids. For this purpose, cDNA fragment encoding AtRbcX1 protein truncated by 46 first amino acids and cDNA fragment encoding AtRbcX2 peptide truncated by 78 first amino acids were amplified using rbcX1prFw (AAACATATGTATGTTCCCGGCTTTGG, *Nde*I site underlined), rbcX1prRv (AAAGGATCCTTTCACTTATCAGAATCG, *Bam*HI site underlined) primers or rbcX2prFw (AAACATATGGAGGATGTTGCTGGTAATTAC, *Nde*I site underlined), and rbcX2prRv (AAAGGATCCCTATTACCTTG AGTTTGTGT, *Bam*HI site underlined) primers, respectively.

For co-expression experiments, cDNA fragment of *AtRbcX1* encoding processed protein was amplified by PCR using rbcX1Fw (AAAGAGCTCAGAAGGAGATATACA TATGTATG, *Sac*I site underlined) and rbcX1Rv (AAATCTAGAGTTTCACTTATCAGAATCGG, *Xba*I site underlined) primers and pET21rbcX1 vector as a template. The sequence of *AtRbcX2* truncated by first 78 amino acids encoding fragment was amplified using rbcX2Fw (AAA GAGCTCAGAAGGAGATATACATATGGTG, *Sac*I site underlined) and rbcX2Rv (AAATCTAGAGCCTATTAC CTTGAGTTTGTG, *Xba*I site underlined) primers. Both PCR products digested with *Sac*I and *Xba*I were cloned into pCM18 vector (Tarnawski et al. 2008a, previously named pUC18CM) giving pCMrbcX1 and pCMrbcX2 plasmids.

Expression plasmid pET21X1C62L/C87A encoding AtRbcX1 with replaced cysteines was constructed by subsequent two-step introduction of C62L and C87A substitutions into pET21rbcX1pr plasmid. Both substitutions were introduced using QuickChange Lightning Site-Directed Mutagenesis Kit (Stratagene) according to manufacturer's instruction and following primers: C62LFw (GTGA CGGTGATAAATTCTTAGCCACTCTCATGCGTCGC), C62LRv (GCGACGCATGAGAGTGGCTAAGAATTTAT CACCGTCAC), C87AFw (GAGGTACGGTCTGCTTA TGCAAAAAACGATTTCGAATGGG) and C87ARv (CC CATTCGAAATCGTTTTTTGCATAAGCAGACCGTACC TC3). Underlined nucleotides indicate introduced substitutions. All plasmids were verified by DNA sequencing.

Cell cultures

To study the co-expression of Rubisco large and small subunits with AtRbcX proteins, DH5 α *E. coli* cells were co-transformed with pUC18rbcLS (Tarnawski et al. 2008a) and either one of the pCMrbcX1 and pCMrbcX2 plasmids. Cells were cultured in LB medium supplemented with ampicillin (100 μg/ml) and chloramphenicol (25 μg/ml) at 37°C to $OD_{600} \sim 0.6$–0.7. Expression of proteins encoded by above-indicated plasmids was induced with 0.5 mM IPTG followed by growth for another 16–17 h.

To overexpress the mature AtRbcX proteins, *E. coli* Rosetta strain was transformed with pET21rbcX1pr, pET21rbcX2pr or pET21rbcX1C62L/C87A plasmid. Culture conditions were as the ones described for co-expression experiment, except that IPTG induction was carried out at 15°C in case of pET21rbcX1pr and pET21rbcX2pr transformed cells. After 3 h of expression, *E. coli* cells were pelleted by centrifugation at 3,000*g* for 10 min at 4°C and stored at −20°C for further analysis. Rosetta™ (Novagen) strain was chosen because of high frequency of rare codons present in both genes to be expressed.

AGL-1 *Agrobacterium tumefaciens* cells transformed with pCam-rbcX1ST or pCam-rbcX2ST plasmids were grown in MG/L medium (250 mg/l KH_2PO_4, 100 mg/l NaCl, 100 mg/l $MgSO_4 \times 7\ H_2O$, 5 g/l tryptone, 2.5 g/l yeast extract, 5 g/l mannitol, 1 g/l L-glutamic acid, 1 mg/l biotin) supplemented with ampicillin (100 μg/ml) and kanamycin (50 μg/ml) at 30°C.

Electrophoresis and Western blotting analysis

Crude extracts from *E. coli* culture, as well as extracts of *Arabidopsis* chloroplasts were separated by Tricine-PAGE (10% gel) according to Schagger and von Jagow (1987). For Western blotting, proteins were transferred on nitrocellulose or PVDF membrane and probed with anti-RbcL (Agrisera, dilution 1:5,000) and anti-Strep Tag II (GenScript, dilution 1:1,000) antibodies for 2 h at room temperature. Immunobloting and detection were carried out as described previously (Szczepaniak and Cramer 1990).

Protein concentration measurement

Protein concentration for electrophoresis was measured using Roti-Nanoquant reagent (Roth) according to manufacturer's instruction with bovine serum albumin as a standard. Protein concentrations for CD spectra were established on the basis of A_{280} of AtRbcX1 and AtRbcX2 signal sequence-lacking peptides denatured in 6 M guanidine hydrochloride. Molar extinction coefficients of processed AtRbcX proteins were calculated on the basis of amino acid sequences using Peptide Properties Calculator (http://www.basic.northwestern.edu/biotools/proteincalc.html).

Recombinant protein purification

To purify recombinant AtRbcX proteins, harvested *E. coli* cells were disrupted by sonication in a 20 mM Tris–HCl buffer, pH 8.0, containing 100 mM NaCl, 1 mM EDTA, 1 mM PMSF and 20 mM β-mercaptoethanol (β-mercaptoethanol was omitted in case of AtRbcX1C62L/C87A purification), centrifuged at 20,000*g* for 30 min at 4°C and supernatants were collected. AtRbcX1 and AtRbcX1C62L/C87A proteins were subjected to ammonium sulfate precipitation between 20 and 25% of saturation. Additional gel filtration on Superdex 75 column in a 20 mM Tris–HCl buffer, pH 8.0 containing 200 mM NaCl and 20 mM β-mercaptoethanol was performed in case of AtRbcX1. AtRbcX2 protein was purified in three steps which consisted of ammonium sulfate precipitation up to 30% of saturation, anion exchange chromatography on MonoQ column (GE Healthcare) equilibrated with 20 mM Tris–HCl, pH 8.5 and 20 mM β-mercaptoethanol (proteins were eluted with a gradient of 0–1 M NaCl in Tris buffer) and final gel filtration on Superdex 75 column in 20 mM Tris–HCl buffer, pH 8.5 containing 300 mM NaCl and 20 mM β-mercaptoethanol.

CD spectroscopy

Measurements of CD spectra were performed with a Jasco J-815 spectropolarimeter. Prior to the measurement, proteins were dialyzed against 5 mM phosphate buffer, pH 8.0 and then diluted to ca. 0.1 mg/ml. CD spectra were obtained in a range of 185–260 nm at 22°C.

Rubisco carboxylase assay

The carboxylase activity of Rubisco-containing extracts was determined at 30°C as the RuBP-dependent incorporation of $^{14}CO_2$ into acid-stable 3-phosphoglyceric acid (PGA) according to Whitman and Tabita (1976). Prior to the assay, the enzyme was fully activated by incubation in 50 mM Bicine-NaOH pH 8.0 buffer containing 20 mM $MgCl_2$, 20 mM $NaH^{14}CO_3$ (specific activity 1 Ci/mol) and 2 mM DTT at 30°C for 30 min. The final volume of the reaction mixture was 0.5 ml. The carboxylase reaction was initiated by the addition of RuBP to the final concentration of 0.4 mM and was terminated by adding 2 M HCl (0.1 ml of reaction mixture per 0.5 ml 2 M HCl). Samples were dried and the residues were resuspended in 0.5 ml water and mixed with 4.5 ml of scintillation fluid. The incorporation of $^{14}CO_2$ into PGA was quantified by liquid scintillation counting (LS-6500 Liquid Scintillation Counter, Beckman). Specific activity was expressed as micromoles of $^{14}CO_2$ fixed per minute per milligram of protein in crude extract.

Arabidopsis transformation

Arabidopsis thaliana (Col-0) plants were transformed with pCam-rbcX1ST and pCam-rbcX2ST plasmids using agroinfiltration according to Davis et al. (2009). Selection of transgenic seeds was conducted on Murashige & Skoog Basal Medium (Sigma) supplemented with 1.5% sucrose and hygromycin (25 μg/ml), solidified with 1.5% agar. The presence of transgene in hygromycin-resistant plantlets was confirmed by PCR using pC1302Fw (CCTTCGCAAGACCCTTCCTCTA) and pC1302Rv (GACCGGCAACAGGATTCAATCT) primers complementary to the region flanking genes introduced to pCambia1302 vector.

Isolation and fractionation of chloroplasts from *Arabidopsis thaliana*

Intact chloroplasts from ca. 6–8-week-old wild type and transgenic *A. thaliana* plants were purified according to Seigneurin-Berny et al. (2008). Chlorophyll concentration was determined by spectrophotometry after solubilization in acetone. Chloroplasts were disrupted by 10 min incubation on ice in lysis buffer (62.5 mM Tris–HCl pH 7.5, 2 mM $MgCl_2$) and then centrifuged at 10,000*g* for 10 min at 4°C. Supernatants contained stromal proteins whereas intact thylakoids were present in pellet fractions. For further washing of peripherial proteins, thylakoid pellets were resuspended in 20 mM CAPS buffer, pH 12 or lysis buffer containing 1 M NaCl or 0.05% Triton X-100, incubated for 1 h on ice and then centrifuged at 145,000*g* for 1 h at 4°C.

Isolation of Strep-Tagged proteins from transgenic *Arabidopsis thaliana* plants

Approximately 10 g of leaves from X1ST or X2ST *Arabidopsis* transformants were ground in liquid nitrogen and then resuspended in disruption buffer (DB; 50 mM phosphate buffer, pH 8.0, 300 mM NaCl, 5 mM EDTA, 10 mM

DTT, 0.5% Triton X-100, 1 mM PMSF). After centrifugation at 25,000*g* for 30 min at 4°C, supernatant was loaded onto previously DB-equilibrated Strep-Tactin Superflow Plus resin (Qiagen). Loaded resin was washed with 10 volumes of wash buffer (WB, 50 mM phosphate buffer, pH 8.0, 300 mM NaCl, 2.5 mM EDTA, 2 mM DTT, 0.05% Triton X-100). Bound proteins were eluted with WB containing 5 mM biotin and then TCA-precipitated.

Protein identification by mass spectrometry

TCA-precipitated proteins were resuspended in 10 mM Tris–HCl pH 8.0 and subjected to Tricine-PAGE electrophoresis and Coomassie staining. Bands present in polyacrylamide gel were cut off, trypsin-digested and subjected to mass spectroscopy analysis at Mass Spectroscopy Laboratory of Biophysics and Biochemistry Institute of Polish Academy of Science (Warsaw, Poland).

N-terminal amino acid sequencing

N-terminal protein sequence analysis was performed at the BioCentrum Ltd. facility (Krakow, Poland). In short, TCA-precipitated proteins eluted from Strep-Tactin Superflow Plus resin were resuspended in 10 mM Tris–HCl pH 8.0, subjected to Tricine-PAGE electrophoresis and transferred to PVDF membrane. Seventeen kDa bands corresponding to the AtRbcX polypeptides were cut off from the PVDF membrane and subjected to the Edman degradation procedure in order to establish the sequences of N-termini. The sequentially detached phenylthiohydantoin derivatives of amino acids were identified using a Procise 491 (Applied Biosystems) automatic sequence analysis system.

Acknowledgments This work was supported by grant NN303 415637 from the Ministry of Science and Higher Education, Poland.

References

Belanger FC, Leustek T, Chu B, Kriz AL (1995) Evidence for the thiamine biosynthetic pathway in higher-plant plastids and its developmental regulation. Plant Mol Biol 29(4):809–821

Bologna G, Yvon C, Duvaud S, Veuthey AL (in press) N-terminal myristoylation predictions by ensembles of neural networks. Proteomics

Bowes G, Ogren WL, Hageman RH (1971) Phosphoglycolate production catalysed by ribulose diphosphate carboxylase. Biochem Biophys Res Commun 45:716–722

Brutnell TP, Sawers RJ, Mant A, Langdale JA (1999) BUNDLE SHEATH DEFECTIVE2, a novel protein required for post-translational regulation of the *rbcL* gene of maize. Plant Cell 11(5):849–864

Chen GG, Jagendorf AT (1994) Chloroplast molecular chaperone-assisted refolding and reconstitution of an active multisubunit coupling factor CF1 core. Proc Natl Acad Sci USA 91: 11497–11501

Cleland WW, Andrews TJ, Gutteridge S, Hartman FC, Lorimer GH (1998) Mechanism of RuBisCO: the carbamate as general base. Chem Rev 98:549–562

Cloney LP, Bekkaoui DR, Hemmingsen SM (1993) Co-expression of plastid chaperonin genes and a synthetic plant Rubisco operon in *Escherichia coli*. Plant Mol Biol 23:1285–1290

Cohen I, Knopf JA, Irihimovitch V, Shapira M (2005) A proposed mechanism for the inhibitory effects of oxidative stress on Rubisco assembly and its subunit expression. Plant Physiol 137(2):738–746

Dalbey RE, Lively MO, Bron S, van Dijl JM (1997) The chemistry and enzymology of the type I signal peptidases. Protein Sci 6(6):1129–1138

Davis AM, Hall A, Millar AJ, Darrah C, Davis SJ (2009) Protocol: Streamlined sub-protocols for floral-dip transformation and selection of transformants in *Arabidopsis thaliana*. Plant Methods 5:3

Emanuelsson O, Brunak S, von Heijne G, Nielsen H (2007) Locating proteins in the cell using TargetP, SignalP, and related tools. Nat Protoc 2:953–971

Emlyn-Jones D, Woodger FJ, Price GD, Whitney SM (2006) RbcX can function as a RuBisCO-chaperonin, but is not essential in *Synechococcus* PCC7942. Plant Cell Physiol 47:1630–1640

Flexas J, Medrano H (2002) Drought-inhibition of photosynthesis in C3 plants: stomatal and non-stomatal limitations revisited. Ann Bot 89(2):183–189

Goloubinoff P, Gatenby AA, Lorimer GH (1989) GroE heat-shock proteins promote assembly of foreign prokaryotic ribulose bisphosphate carboxylase oligomers in *Escherichia coli*. Nature 337:44–47

Higgins DG, Thompson JD, Gibson TJ (1996) Using CLUSTAL for multiple sequence alignments. Methods Enzymol 266:383–402

Hofmann K, Stoffel W (1993) TMbase–a database of membrane spanning proteins segments. Biol Chem Hoppe Seyler 374:166

Kohzuma K, Cruz JA, Akashi K, Hoshiyasu S, Munekage YN, Yokota A, Kramer DM (2009) The long-term responses of the photosynthetic proton circuit to drought. Plant Cell Environ 32(3):209–219

Krogh A, Larsson B, von Heijne G, Sonnhammer EL (2001) Predicting transmembrane protein topology with a hidden Markov model: application to complete genomes. J Mol Biol 305:567–580

Li L-A, Tabita FR (1997) Maximum activity of recombinant ribulose-1, 5-bisphosphate carboxylase/oxygenase of *Anabaena* sp. strain CA requires the product of the *rbcX* gene. J Bacteriol 179: 3793–3796

Liu C, Young AL, Starling-Windhof A, Bracher A, Saschenbrecker S, Vasudeva Rao B, Vasudeva Rao K, Berninghausen O, Mielke T, Hartl FU, Beckmann R, Hayer-Hartl M (2010) Coupled chaperone action in folding and assembly of hexadecameric Rubisco. Nature 463:197–202

Muehlbauer SK, Eichacker LA (1999) The stromal protein large subunit of ribulose-1, 5-bisphosphate carboxylase is translated by membrane-bound ribosomes. Eur J Biochem 261:784–788

Mueller-Cajar O, Whitney SM (2008) Evolving improved *Synechococcus* Rubisco functional expression in *Escherichia coli*. Biochem J 414:205–214

Onizuka T, Endo S, Akiyama H, Kanai S, Hirano M, Yokoya A, Tanaka S, Miyasaka H (2004) The rbcX gene product promotes the production and assembly of ribulose-1, 5-bisphosphate carboxylase/oxygenase of Synechococcus sp. PCC7002 in Escherichia coli. Plant Cell Physiol 45:1390–1395

Ren J, Wen L, Gao X, Jin C, Xue Y, Yao X (2008) CSS-Palm 2.0: an updated software for palmitoylation sites prediction. *Protein Engineering*. Design Select 21(11):639–644

Saschenbrecker S, Bracher A, Vasudeva Rao K, Vasudeva Rao B, Hartl FU, Hayer-Hartl M (2007) Structure and function of RbcX, an assembly chaperone for hexadecameric rubisco. Cell 129: 1189–1200

Schagger H, von Jagow G (1987) Tricine-sodium dodecyl sulfate-polyacrylamide gel electrophoresis for the separation of proteins in the range from 1 to 100 kDa. Anal Biochem 166:368–379

Seigneurin-Berny D, Salvi D, Dorne AJ, Joyard J, Rolland N (2008) Percoll-purified and photosynthetically active chloroplasts from Arabidopsis thaliana leaves. Plant Physiol Biochem 46(11): 951–955

Small I, Peeters N, Legeai F, Lurin C (2004) Predotar: a tool for rapidly screening proteomes for N-terminal targeting sequences. Proteomics 4(6):1581–1590

Smith SA, Tabita FR (2003) Positive and negative selection of mutant forms of prokaryotic (cyanobacterial) ribulose-1, 5-bisphosphate carboxylase/oxygenase. J Mol Biol 331:557–569

Szczepaniak A, Cramer WA (1990) Tylakoid membrane protein topography-location of the termini of the chloroplast cytochrome b6 on the stromal side of the membrane. J Biol Chem 265: 17720–17726

Tarnawski M, Gubernator B, Kolesinski P, Szczepaniak A (2008a) Heterologous expression and initial characterization of recombinant RbcX protein from Thermosynechococcus elongatus BP-1 and the role of RbcX in RuBisCO assembly. Acta Biochim Pol 55(4):777–785

Tarnawski M, Krzywda S, Szczepaniak A, Jaskolski M (2008b) Rational 'correction' of the amino-acid sequence of RbcX protein from the thermophilic cyanobacterium Thermosynechococcus elongatus dramatically improves crystallization. Acta Crystallogr Sect F Struct Biol Cryst Commun. 64(Pt 9):870–874

Whitman W, Tabita FR (1976) Inhibition of D-ribulose 1, 5–bisphosphate carboxylase by pyridoxal 5′-phosphate. Biochem Biophys Res Commun 71:1034–1039

Whitney SM, von Caemmerer S, Hudson GS, Andrews J (1999) Directed mutation of the Rubisco large subunit of tobacco influences photorespiration and growth. Plant Physiol 121:579–588

Whitney SM, Kane HJ, Houtz RL, Sharwood RE (2009) Rubisco oligomers composed of linked small and large subunits assemble in tobacco plastids and have higher affinities for CO2 and O2. Plant Physiol 149(4):1887–1895

Wostrikoff K, Stern D (2007) Rubisco large-subunit translation is autoregulated in response to its assembly state in tobacco chloroplast. PNAS 104(15):6466–6471

Zhang XP, Glaser E (2002) Interaction of plant mitochondrial and chloroplast signal peptides with the Hsp70 molecular chaperone. Trends Plant Sci 7(1):14–21